Combined Theoretical and FTIR Spectroscopic Studies on Hydrogen Adsorption on the Zeolites Na−FER and K−FER

C. Otero Areán,[†] G. Turnes Palomino,[†] E. Garrone,[‡] D. Nachtigallová,[§] and P. Nachtigall*[,§]

Departamento de Química, Universidad de las Islas Baleares, E-07122 Palma de Mallorca, Spain, Dipartimento di Scienza dei Materiali ed Ingegneria Chimica, Politecnico di Torino, I-10126 Turin, Italy, and Institute of Organic Chemistry and Biochemistry, Academy of Sciences of the Czech Republic and Center for Biomolecules and Complex Molecular Systems, Flemingovo n. 2, CZ-16610 Prague, Czech Republic

Received: September 14, 2005; In Final Form: November 3, 2005

The interaction between molecular hydrogen and the alkali-metal-exchanged zeolites Na−FER and K−FER at a low temperature was investigated by combining variable-temperature infrared spectroscopy and theoretical calculations by using a periodic DFT model. The experimentally determined values of standard adsorption enthalpy, $\Delta H°$, were −6.0 (±0.8) and −3.5 (±0.8) kJ mol^{-1} for Na−FER and K−FER, respectively. These results were found to be in agreement with corresponding $\Delta H°$ values obtained from calculations on the periodic model. Two types of alkali-metal cation sites in FER were found: channel intersection sites and channel wall sites. Calculations showed a similar interaction energy for both site types, and similar structures of adsorption complexes. Up to two dihydrogen molecules can be physisorbed on the alkali-metal cation located on the intersection of two channels, while only one H_2 molecule is physisorbed on the cation at the channel wall site. The adsorption enthalpies of H_2 on alkali-metal-exchanged FER are significantly smaller than those found previously for the MFI-type zeolites Na−ZSM-5 and K−ZSM-5, which is likely due to a difference in the alkali-metal cation coordination in the two zeolite frameworks.

1. Introduction

Gas adsorption on zeolites and related microporous materials is at the basis of several technological processes involving, inter alia, gas separation (based on differences in adsorption strength among components of a gas mixture), gas storage, and atmosphere pollution control. Regarding hydrogen, examples can be found in the use of zeolites in pressure-swing adsorption processes used for separation of this gas from a variety of feedstocks, such as refinery off-gas and hydrogen-rich gas from steam reforming of hydrocarbons. On the other hand, it should be noted that zeolites are among the adsorbents proposed as candidates for large-scale (reversible) hydrogen storage in cryogenically cold vessels.[1−3] This last subject constitutes a present-day strategic issue in the energy sector in view of the potential use of hydrogen as an energy vector in a sustainable (and cleaner) energy scenario.

The foregoing processes involve weak gas−solid interactions, giving rise to hydrogen physisorption. The energy balance in such weak interactions is expected to be in the range of 2−20 kJ mol^{-1}, thus posing demanding requirements on experimental measurements. In particular, adsorption calorimetry is cumbersome to perform in the case of hydrogen physisorption due to both the low temperature required for significant adsorption to take place and the small amount of heat evolved. A convenient alternative is the use of variable-temperature FTIR spectroscopy, which, under favorable circumstances, can advantageously be used for experimental thermodynamic studies on weak solid−gas interactions.[4−6]

Variable-temperature FTIR spectroscopy has recently been applied, in the same way as done here, for experimentally determining the standard adsorption enthalpy of hydrogen on the zeolites M^+−ZSM-5 (M = Li, Na, K).[7−9] Analysis of such experimental results can substantially benefit from detailed quantum chemical studies on the systems under consideration. Interaction of H_2 with bare alkali-metal cations was recently investigated theoretically.[10] However, to understand the changes in adsorption enthalpy due to a different zeolite structure, so as to compare directly experimental and theoretical results, a reliable model describing the significant part of the zeolite framework must be adopted. Ideally, a periodic model accounting for the H_2 interactions with the entire framework should be used. However, the rather large unit cell of ZSM-5 together with the large number of distinguishable framework T positions make this zeolite computationally too demanding for systematic investigation at the periodic DFT level. By contrast, zeolites having a relatively small unit cell can be treated at a periodic density functional theory (DFT) level, where framework topology is fully respected, hence, giving a more realistic description of the gas−solid interaction than what can be attained by simple considerations on cluster models. This is the main reason why Na−FER and K−FER were chosen for the present study.

2. Materials and Methods

2.1. Experimental. The starting ammonium form of the ferrierite zeolite (Si/Al = 8.6) used in this study was supplied by Research Institute of Inorganic Chemistry, Ústí nad Labem. From the parent zeolite, the sodium- and potassium-exchanged samples (having 100% exchange level) were obtained by ion exchange repeated three times with 0.5 M aqueous solutions of

* Corresponding author. E-mail: petr.nachtigall@uochb.cas.cz. Telephone: +420-220-410-314. Fax: +420-220-410-320.

[†] Departamento de Química, Universidad de las Islas Baleares.

[‡] Dipartimento di Scienza dei Materiali ed Ingegneria Chimica, Politecnico di Torino.

[§] Institute of Organic Chemistry and Biochemistry, Academy of Sciences of the Czech Republic.

10.1021/jp055190k CCC: $33.50
Published on Web 12/08/2005

NaCl and KCl, respectively. Powder X-ray diffraction of the exchanged samples showed good crystallinity in both cases, and all diffraction lines present in the diffractograms corresponded to the FER structure type. Complete ion exchange was checked by the absence of IR absorption bands corresponding to either the ammonium ion or the Brønsted acid Si(OH)Al group, which would be generated during thermal activation (see below) of the zeolite samples if total exchange of the alkali-metal ions for ammonium did not take place in the parent NH_4−FER material.

For IR spectroscopic measurements, thin self-supported wafers of the zeolite samples were prepared and activated (outgassed) in a dynamic vacuum (residual pressure $< 10^{-4}$ Torr) for 3 h at 700 K inside an IR cell,[11] which allowed in situ sample activation, gas dosage, and variable-temperature IR spectroscopy to be carried out. For each sample, after running the blank spectrum of the zeolite wafer at 77 K, the cell was dosed with hydrogen, it was then closed, and IR spectra were recorded at several fixed temperatures, within the range of 85 to 120 K, while simultaneously registering sample temperature and hydrogen equilibrium pressure inside the cell. A platinum resistance thermometer and a capacitance pressure gauge were used for this purpose. The precision of these measurements was about ±2 K and $\pm 2 \cdot 10^{-2}$ Torr, respectively. Transmission FTIR spectra were recorded, at 3 cm^{-1} resolution, using a Bruker IFS66 spectrometer.

2.2. Calculations. Calculations were performed by using the periodic DFT method, employing the Perdew−Burke−Erzenhofer (PBE) exchange-correlation functional[12,13] and the projector-augmented wave approximation (PAW) of Blöchl, as adapted by Kresse and Joubert.[14,15] The plane wave basis set, with a kinetic energy cutoff of 400 eV, was used. Brillouin zone sampling was restricted to the Γ point. Calculations were performed by using the VASP program.[16−19]

The (orthorhombic) unit cell of ferrierite (I_{mmm} space group) contains 36 T atoms (Si or Al) and 72 O atoms. The equilibrium volume of the all-silica FER unit cell (cell parameters a = 19.1468, b = 14.3040, and c = 7.5763 Å, volume 2076.70 Å^3) fitted previously[20] was used for all calculations on H_2/M^+−FER. One framework Si atom was replaced by aluminum, and the charge was compensated by a Na^+ or a K^+ cation. Calculations of H_2 adsorption enthalpies were carried out for the Al atom in the T2 and T3 positions (the numbering scheme of ref 21 was adopted).[22]

Calculations on cluster models were also performed by using the PBE exchange-correlation functional and at the MP2 level with the aug-cc-pVTZ basis set.[23,24] Calculations with the atom-centered basis set were carried out with the Gaussian03 program suite.[25] C_{2v} symmetry constraints were applied in all calculations with cluster models, and interaction energies were corrected for the basis set superposition error.[26] Zero-point energy (ZPE) corrections were calculated within the harmonic approximation for the 1-T cluster model ($Al(OH)_4^-M^+$ cluster). The sum of the electronic interaction energy and ZPE gives the internal energy change at 0 K, $\Delta U^0(0)$. Experimental determination of $\Delta H°$ was carried out at temperatures around 100 K; therefore, $\Delta U^0(100)$ was evaluated from the partition function by considering six degrees of freedom, and the ideal gas equation was used for the transition from internal energy change to enthalpy change ($\Delta H°(T) = \Delta U^0(T) + pV = \Delta U^0(T) + RT$). Details are given in Section 3.2.

3. Results

3.1. Coordination of Alkali-Metal Cations in FER. The location of alkali-metal cations (Na^+ and K^+) in FER was investigated systematically, considering the framework Al at all four distinguishable positions and all possible coordinations of metal cations in the vicinity of the framework aluminum atom. The most stable site for Na^+ is the channel wall site (type I site according to the notation introduced in ref 27) when the framework Al atom is in a T3 position. This "M7/T3" site is located in the main channel of FER.[28] The second most stable site found for Na^+ is the channel intersection site (type II site) in the eight-member ring window when the framework Al atom is in a T2 position. This site, denoted "I2/T2", is on the intersection of main and perpendicular channels. The M7/T3 and I2/T2 sites where also identified as the most stable sites of K^+ in FER.

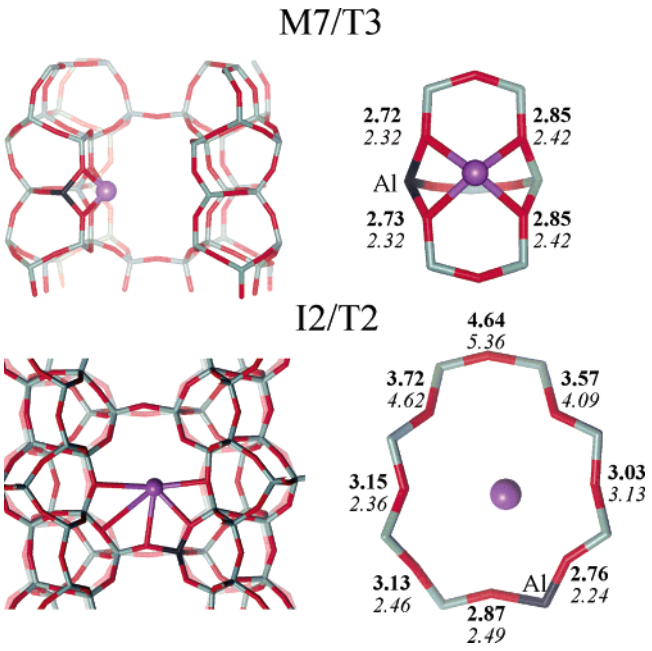

Figure 1. The most stable cation sites in FER (left-hand side). In the M7/T3 site, the cation (K^+) is located on top of a six-member ring on the wall of the main channel; in the I2/T2 site, this cation is at the eight-member ring entrance window of the perpendicular channel. Distances between cation and closest framework oxygen atoms are shown, in bold for K^+ and italic for Na^+, on the right-hand side.

Both of these sites are depicted in Figure 1. In M7/T3 sites, the K^+ ion is coordinated to two oxygen atoms of an AlO_4 tetrahedron and two oxygen atoms of a SiO_4 tetrahedron, having a coordination number CN = 4. In I2/T2 sites, the K^+ ion is located nearly in the center of the eight-member ring entrance of the perpendicular channel, and it is coordinated to five framework oxygen atoms (CN = 5). Note that the K^+ and Na^+ ions are considered to be coordinated to the framework oxygen atom when the metal−oxygen distance is shorter than 3.18 and 2.73 Å, respectively.[29] The Na^+ cation is coordinated to two framework oxygen atoms of an AlO_4 tetrahedron and two framework oxygen atoms of an SiO_4 tetrahedron (CN = 4) in both M7/T3 and I2/T2 sites, respectively.

3.2. Calculation of Dihydrogen Adsorption Enthalpy. To compare the calculated interaction energies (electronic interaction energy) with the experimental adsorption enthalpy values, it is necessary to include several corrections: the effect of ZPE, thermal contribution, and the pV term. In the majority of applications, the ZPE is calculated within the harmonic approximation, the thermal effect on vibrational degrees of freedom is neglected, and for gas phase molecules, $RT/2$ is taken for each degree of freedom. The pV term is simply approximated by RT. All of these effects are relatively small for strong adsorption; Δ(ZPE) is typically ∼10 kJ mol^{-1}, and the other

TABLE 1: Harmonic Frequencies, ω, of Relevant Normal Modes and Energy Corrections Calculated at PBE/aug-cc-pVTZ Level for the 1-T Cluster Model

normal mode[a]	$Na^+Al(OH)_4^-H_2$	$K^+Al(OH)_4^-H_2$
	ω[b]	
H_2 in plane (B_2)	21	8
H_2 out of plane (B_1)	28	7
H_2 rotation (A_2)	107	9
M^+-H symmetric stretching (A_1)	233	136
M^+-H asymmetric stretching (B_2)	461	306
H−H stretching (A_1)	4272	4296
H_2 gas phase[c]	4317	4317
	Energy Corrections[d]	
Δ(ZPE)	5	2.7
$\Delta U^0(100) - \Delta U^0(0)$[e]	−0.2	0.6
$\Delta E^{el} - \Delta H°(100)$[f]	4.0	2.5

[a] Six normal modes describing the motion of hydrogen atom, symmetry given in parentheses. [b] Harmonic frequency in cm^{-1}. [c] Harmonic frequency of H−H stretching mode for gas-phase H_2. [d] In kJ mol^{-1}. [e] $^5/_2RT$ used for rotational and translational degrees of freedom, thermal effect due to vibrational motion described in Section 3.2. [f] Sum of Δ(ZPE) and thermal energy minus pV term.

two effects are even smaller. Therefore, this approximate approach is sufficiently accurate for strongly interacting systems. However, for only weakly interacting systems (as in this study), the electronic interaction energy, Δ(ZPE), and thermal energy are all of the same order. Note that, in a weakly interacting system, some of the vibrational modes have a very low energy and vibrational excited states can be thermally populated.

The thermal contributions to adsorption energy (enthalpy) were calculated only with the 1-T cluster model, employing C_{2v} symmetry constraints and harmonic approximation. Calculations were carried out at the PBE/aug-cc-pVTZ level. The change of ZPE due to H_2 adsorption calculated for all degrees of freedom is essentially the same as that calculated for only six degrees of freedom of the H_2 molecule (six vibrational degrees for adsorption complex and one, two, and three vibrational, rotational, and translational degrees of freedom for gas-phase H_2, respectively). A representative temperature of 100 K was assumed because experimental measurements were carried out around this temperature value. Vibrational frequencies of the six normal modes describing the motion of two hydrogen atoms are summarized in Table 1 for $H_2-NaAl(OH)_4$ and $H_2-KAl(OH)_4$ complexes. The effect of temperature on the vibrational degrees of freedom was calculated from the vibrational partition function of a harmonic oscillator:[30]

$$E_v(100) - E_v(0) = \sum_i \frac{N_A k \Theta_v^{\,i}}{e^{\Theta_v^{i}/T} - 1} \qquad (1)$$

where $\Theta_v^{\,i} = h\nu_i/k$, ν_i is the energy of ith vibrational mode, and N_A, k, and h are Avogadro's number, Boltzmann, and Planck constants, respectively. The effects of ZPE and thermal energy are summarized in Table 1, together with the overall energy change when going from electronic interaction energy, ΔE^{el}, to $\Delta H°$ (100). The adsorption enthalpy is increased by rotational and translational degrees of freedom of the gas-phase H_2 molecule by 2.1 kJ mol^{-1} for adsorption on both cations. Thermal population of low-energy vibrational states decreases adsorption enthalpy by −1.8 and −2.7 kJ mol^{-1} for Na−FER and K−FER systems, respectively. These effects, calculated with the 1-T cluster model, were used for correction of all calculated electronic interaction energies of H_2/M^+-FER systems.

3.3. Interaction of H_2 with M^+-FER. The interaction of H_2 with M^+-FER was computationally studied for the two energetically most stable sites of Na^+ and K^+. In addition, interaction of H_2 with the simple cluster model $Al(OH)_4^-M^+$ was also studied. This simple cluster is termed 1-T because it contains only a single framework T atom. For comparison, bare metal cations (0-T model) were also considered. Results obtained with these two models are reported in Table 2, along with the results obtained by using a more sophisticated periodic model (FER).

The interaction of H_2 with the alkali-metal cation is dominated by the polarization term.[31] Accordingly, the strongest interaction was found for H_2 and a bare metal cation (0-T model). When the alkali-metal cation is located in the vicinity of an AlO_4^- tetrahedron, the charge on the metal cation is partially reduced and the interaction with H_2 becomes significantly weaker (see results for the 1-T cluster model in Table 2). In the case of the K^+ ion, the interaction with H_2 calculated for the 1-T model is close to zero.

Calculations performed on the periodic model gave $\Delta H°$ values that are much smaller than those corresponding to the bare cation (as expected), but larger than those obtained by using the 1-T cluster model (Table 2). For the H_2/Na−FER system, the H_2 adsorption enthalpy results are in the range of −7.0 to −5.2 kJ mol^{-1}, over 2 kJ mol^{-1} greater than that found for the 1-T cluster model. For the H_2/K−FER system, adsorption enthalpies calculated with the periodic model come in the narrow range of −2.8 to −2.2 kJ mol^{-1}, again, some 2 kJ mol^{-1} greater than the corresponding value derived by using the 1-T cluster model.

For all models investigated (0-T, 1-T, and periodic model), the structures having the lowest energy resulted in T-shape adsorption complexes. These complexes were found to be very similar for both (Na^+ and K^+) cations, the only difference being the corresponding M^+-H distance. The H_2 adsorption complex on the channel wall site (M7/T3) is an "on top" T-shape structure, shown in Figure 2a, with H_2 localized approximately in the center of the main channel. Two complexes with similar energies were found on the intersection site (I2/T2), where H_2 can approach the cation either from the main channel side (I2/T2+H_2−M complex) or from the adjacent cavity in the perpendicular channel (I2/T2+H_2−P complex). Interestingly, the metal cation at this intersection site can interact with two hydrogen molecules at the same time (Figure 2b depicts such a complex for the K^+ ion), with the overall interaction energy being almost the sum of the interaction energies of the I2/T2+H_2−M and I2/T2+H_2−P complexes.

The H−H bond length is elongated by only a few thousandths of an angstrom upon interaction with the alkali-metal cation. Note that, in the gas-phase, the H_2 molecule r(H−H) is 0.751 Å at the PBE level using both aug-cc-pVTZ and plane-wave basis sets. It is also apparent from Table 2 that, for the same cation, changes in H−H bond length correlate with the corresponding $H_2\cdots M^+$ interaction energy and also that an increased interaction strength results in a shorter M−H bond distance (Table 2). Finally, it is worthwhile adding that coordination of the metal cation to the zeolite framework was found to be unaltered upon interaction with adsorbed dihydrogen, a result not unexpected on account of the small interaction energy involved.

3.4. Variable Temperature FTIR Spectroscopy: Experimental Determination of the Standard Adsorption Enthalpy and Entropy. Representative variable-temperature FTIR spectra (in the H−H stretching region) of molecular hydrogen adsorbed on Na−FER are depicted in Figure 3a; a single H−H stretching band is seen, centered at 4100 cm^{-1}. For K−FER, the

TABLE 2: Adsorption Enthalpy (kJ mol^{-1}) and Bond Distance (Å) for H_2 Adsorbed on Alkali-Metal Cations, Obtained with Cluster Models and with DFT Calculations on the Periodic Model (FER)

		Na^+			K^+		
		r(H−H)	r(M−H)	$\Delta H°$ (100 K)	r(H−H)	r(M−H)	$\Delta H°$ (100 K)
cluster models							
0-T (M^+H_2)[a]		0.757	2.430	−12.9	0.754	2.944	−5.6
1-T ($M^+Al(OH_4^-)H_2$)		0.754	2.581	−3.2	0.752	3.176	−0.2
FER[b]							
M7/T3+H_2[c]		0.754	2.539, 2.544	−5.2	0.753	3.282, 3.255	−2.2
I2/T2+H_2−M[d]		0.755	2.517, 2.537	−5.4	0.753	3.151, 3.157	−2.8
I2/T2+H_2−P[d]		0.757	2.460, 2.448	−7.0	0.753	3.122, 3.130	−2.6
I2/T2+2 × H_2[e]	M	0.755	2.546, 2.520	−6.0	0.753	3.126, 3.144	−2.6
	P	0.757	2.483, 2.468		0.753	3.133, 3.126	
experiment: $\Delta H°$ (100 K)				−6.0 (±0.8)			−3.5 (±0.8)

[a] Calculations on 0-T model were performed with localized aug-cc-pVTZ basis set. [b] Alkali-metal sites are defined in Figure 1. [c] Adsorption complex of H_2 on the Na^+ cation in M7/T3 site is depicted in Figure 2a. [d] M and P denotes adsorption complexes where H_2 is localized in the main channel and in the cavity of perpendicular channel, respectively. [e] Average adsorption enthalpy, adsorption complex of H_2 on the K^+ cation in I2/T2 site is depicted in Figure 2b.

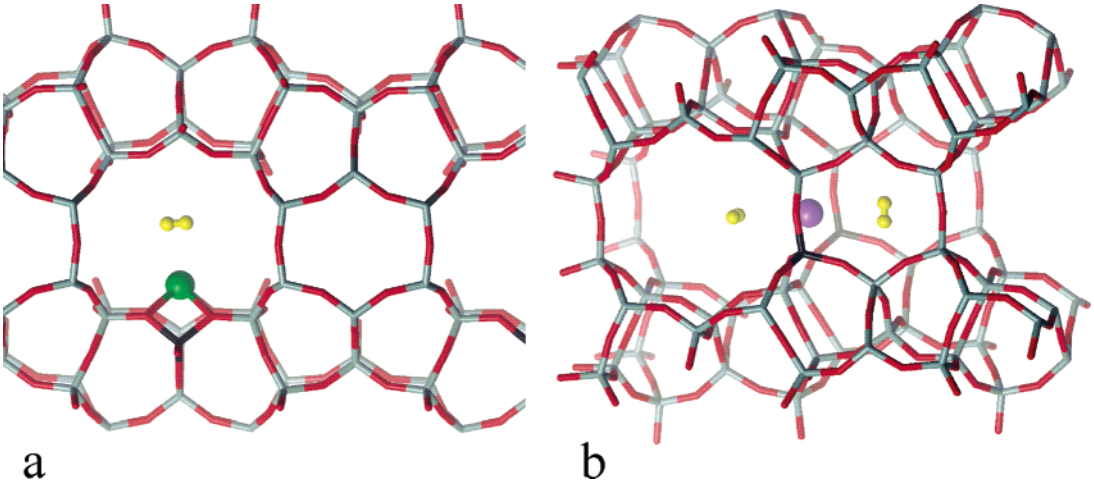

Figure 2. H_2 adsorption complex on Na^+ at M7/T3 site (a) and adsorption complex of two H_2 molecules on K^+ at I2/T2 site (b), viewed along the main channel. Framework O, Si, and Al atoms are depicted in red, gray, and black, respectively. Na, K, and H atoms depicted as green, violet, and yellow balls.

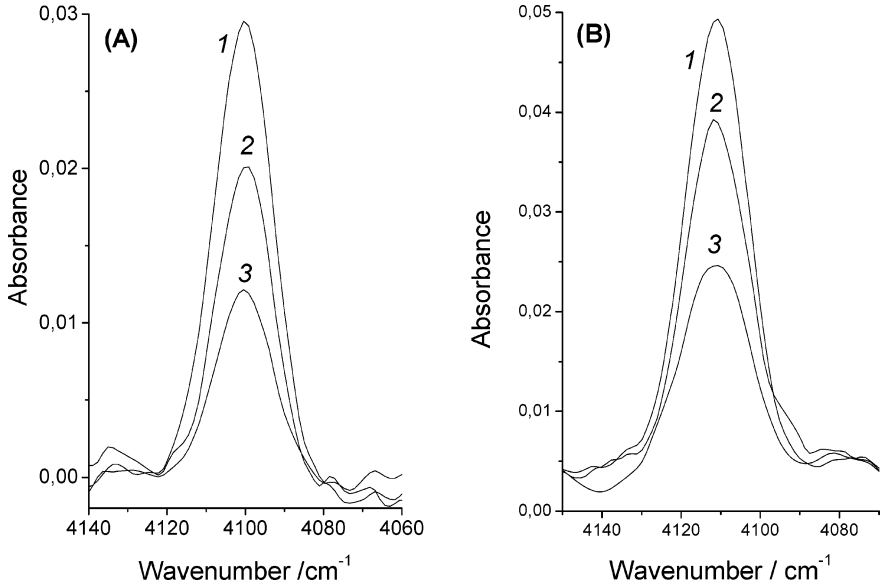

Figure 3. Representative variable-temperature FTIR spectra (zeolite blank subtracted) of dihydrogen adsorbed on (A) Na−FER and (B) K−FER. Temperature (in K) and equilibrium pressure (in Torr) as follows. (A) *1*, 87, 3.86; *2*, 100, 4.14; *3*, 112, 4.66. (B) *1*, 79, 7.22; *2*, 86, 7.56; *3*, 104, 8.27.

corresponding IR spectra (Figure 3b) show the H−H stretching band at 4111 cm^{-1}. The bathochromic frequency shift, from the gas-phase value (4163 cm^{-1}) of the Raman-active H−H stretching vibration of the free H_2 molecule, amounts to −63 and −52 cm^{-1} for dihydrogen adsorbed on Na−FER and K−FER, respectively. A previous account[32] gives the wavenumber value of 4096−4098 cm^{-1} for the H−H stretching mode of dihydrogen adsorbed (at 77 K) on Na−FER, while for Na−

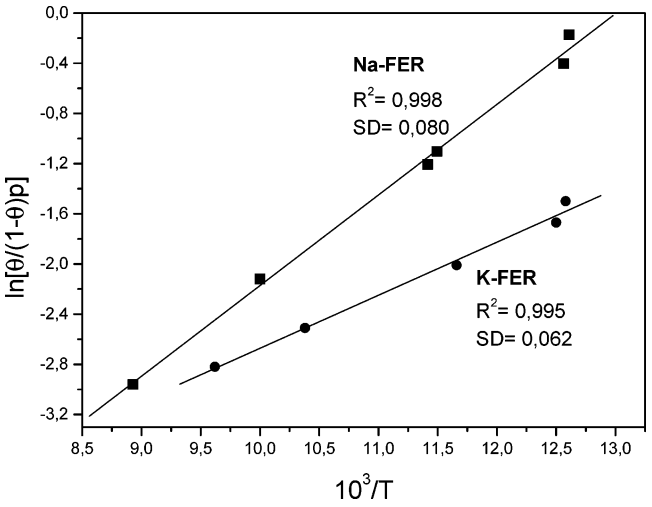

Figure 4. Plot of the left-hand side of eq 5 vs reciprocal temperature for both H_2/Na−FER and H_2/K−FER. *R*, linear regression coefficient; SD, standard deviation.

ZSM-5 and K−ZSM-5, reported values are 4101 and 4112 cm^{-1}, respectively.[8]

From the integrated intensity of variable-temperature IR spectra, and by simultaneously measuring temperature and hydrogen equilibrium pressure, the standard adsorption enthalpy ($\Delta H°$) and entropy ($\Delta S°$) involved in the adsorption process were determined by using the method described in detail elsewhere.[4,5] Briefly, at any given temperature, the integrated intensity of the IR absorption band should be proportional to surface coverage, θ, thus giving information on the activity (in the thermodynamic sense) of both the adsorbed species and the empty adsorbing sites; simultaneously, the equilibrium pressure does the same for the gas phase. Hence the corresponding adsorption equilibrium constant, *k*, can be determined, and the variation of *k* with temperature leads to the corresponding values of adsorption enthalpy and entropy. For deriving these values, integrated band intensity, *A*, temperature, *T*, and hydrogen equilibrium pressure, *p*, were considered to be interrelated by the Langmuir-type eq 2 below:

$$\theta = A/A_M = k(T)p/[1 + k(T)\,p] \qquad (2)$$

where A_M stands for the integrated intensity corresponding to full coverage. Equation 2 can be combined with the well-known van't Hoff equation, 3, to yield eq 4 below:

$$k(T) = \exp[\Delta S^0/R]\,\exp[-\Delta H^0/RT] \qquad (3)$$

$$\ln[A/(A_M - A)p] = (-\Delta H^0/RT) + (\Delta S^0/R) \qquad (4)$$

which can also be written as:

$$\ln[\theta/(1 - \theta)p] = (-\Delta H^0/RT) + (\Delta S^0/R) \qquad (5)$$

Plots of the left-hand side of eq 5 vs reciprocal temperature for all of the experimental measurements obtained for H_2/Na−FER and H_2/K−FER are depicted in Figure 4, which shows a good linear fit of eq 5 for both systems. Note that the needed value of A_M (for which only an approximate estimation was known because experimental points in Figure 4 correspond to a coverage range of $0.2 \le \theta \le 0.6$) was chosen as that giving the best linear fit of eq 5 for all experimental data in each system (see refs 5 and 8 for details). From this A_M value, it was inferred that experimental points in Figure 4 correspond to a coverage range of $0.2 \le \theta \le 0.6$. From the linear plots in Figure 4, the standard enthalpy of adsorption results to be $\Delta H° = -6.0$ kJ mol^{-1} for H_2/Na−FER and $\Delta H° = -3.5$ kJ mol^{-1} for H_2/K−FER, respectively. The corresponding entropy change ($\Delta S°$) is −78 and −57 J mol^{-1} K^{-1} for the sodium- and potassium-exchanged zeolite, respectively. The estimated error limits are about ±0.8 kJ mol^{-1} for enthalpy and ±10 J mol^{-1} K^{-1} for entropy.

4. Discussion

Results to be discussed can be grouped into the following categories: (i) structure and stability of H_2 adsorption complexes, (ii) validity of the experimental determination of the interaction strength of dihydrogen with M^+−FER, (iii) reliability of the theoretical approach, and (iv) comparison between data concerning ferrierite and ZSM-5, both in the alkali-metal-cation exchanged form.

Two types of extraframework alkali-metal-cation sites in FER were found: (i) Sites on the channel wall (type I site: M7/T3), where the alkali-metal cation is coordinated on top of a six-member ring on the channel wall. In this case, a single hydrogen molecule adsorbs on top of the metal cation (Figure 2a). The interaction with a second H_2 molecule is considerably weaker. (ii) Sites on the channel intersection (type II site: I2/T2), where the alkali-metal cation is located on the intersection between two channels. At the I2/T2 site, the hydrogen molecule can be adsorbed from either side of the cation (from the main channel or from the perpendicular channel, Figure 2b), therefore, two H_2 molecules can be adsorbed on a single alkali-metal cation, with an overall interaction energy that is approximately twice of that found for a single H_2 molecule.

The experimental data depicted in Figures 3 and 4 were interpreted by assuming a single homogeneous adsorbing site, giving rise to an ideal Langmuir behavior.[5] By contrast, calculations show that two types of alkali-metal sites exist in FER, one of them capable of adsorbing two H_2 molecules. There are several possible explanations for this apparent contradiction: (i) only one type of site is actually populated in the FER sample used, (ii) H_2 adsorbs only on a single-cation site type at a given H_2 pressure and temperature, or (iii) differences in interaction energy for individual adsorption sites are too small to cause a significant deviation from the ideal Langmuir behavior. Population of alkali-metal-cation sites can be checked by using a different probe molecule. Reported IR spectra of CO adsorbed on Na−FER[32,33] clearly show two distinguishable types of site, characterized by CO stretching frequencies of 2173 and 2157 cm^{-1} (see Figure 1 in ref 33). At given experimental conditions, only the most stable sites are likely to be occupied by adsorbed H_2; however, the interaction energies are very similar for a single H_2 molecule adsorbed on the M7/T3 site and for one or two H_2 molecules adsorbed on the I2/T2 site (Table 2). Hence, the most likely explanation for the experimental results (showing only one IR absorption band and conforming to a Langmuir-type adsorption model) is that, for each system studied, differences in interaction energy for H_2 on M7/T3 and I2/T2 sites are small enough to render these two sites homogeneous (to a first approximation) for adsorbed hydrogen. A further interesting question is whether the nearly perfect equivalence of the H_2 approach by either side of the cation in I2/T2 site, as foreseen by computations, is in any conflict with the assumed Langmuir behavior observed experimentally. This is not so because the same cation provides two independent sites for adsorption and has actually to be counted twice.

Comparison of adsorption enthalpies calculated by using simple cluster models with those computed for the periodic

TABLE 3: Electronic Interaction Energy (Without ZPE Correction) of H_2 with a Bare Cation (0-T model) and with the 1-T Cluster Model $Al(OH)_4^-M^+$ [a]

	Na^+		K^+	
	MP2	PBE	MP2	PBE
0-T	−12.7	−16.5	−6.0	−8.9
1-T	−5.1	−6.7	−2.2	−3.2

[a] Calculations with aug-cc-pVTZ basis set, interaction energy in kJ mol^{-1}.

model shows that the bare cation (0-T model) yields too-large interaction enthalpies, whereas the 1-T cluster model yields too-small values. Adsorption enthalpies calculated with the periodic model for H_2 on Na−FER are in excellent agreement with experimental results. For the H_2/K−FER system, the calculated H_2 adsorption enthalpy (about −2.6 kJ mol^{-1}) is also in good agreement with the corresponding experimental result (−3.5 ± 0.8 kJ mol^{-1}) so that, overall, the calculated enthalpies (as reported in Table 2) agree with the experimentally determined $\Delta H°$ values for both the H_2/Na−FER and H_2/K−FER systems. However, it should be noted that calculation of the adsorption enthalpy with an error limit smaller than about 1 kJ mol^{-1} is (for the vast majority of systems) beyond the capability of modern methods of computational chemistry. Hence, the very satisfactory agreement found between calculated and experimentally determined $\Delta H°$ values could be, to some extent, fortuitous because several possible sources of error are still present, as discussed below.

There are two main sources of uncertainty in the calculations used in this study: (i) reliability of DFT for the description of the electronic structure of the system, and (ii) transition from $\Delta U^0(0)$ to $\Delta H°$ (100). On one hand, the interaction energies calculated with GGA functionals (including the PBE functional) are overestimated; on the other hand, the dispersion attraction is neglected at the DFT level. For H_2 interaction with a bare alkali-metal cation, it has recently been shown[10] that, when a sufficiently large basis set is used, the hybrid B3LYP exchange-correlation functional gives a larger dissociation energy than that obtained at both the MP2 level and from experimental results. Interaction energies (at 0 K, without ZPE correction) calculated by using 0-T and 1-T models, at the PBE/aug-cc-pVTZ and MP2/aug-cc-pVTZ levels, are summarized in Table 3. The H_2 interaction with a bare alkali-metal cation calculated at the PBE level is overestimated, compared to the MP2 level, by −3.8 and −2.8 kJ mol^{-1} for Na^+ and K^+, respectively. However, this difference between PBE and MP2 results becomes smaller for the 1-T cluster model: −1.6 and −1.0 kJ mol^{-1} for Na^+ and K^+, respectively. The role of the dispersion interaction neglected at the DFT level was evaluated on the basis of the symmetry-adapted perturbation theory (SAPT) interaction energy analysis,[34] carried out at the MP2 level. Calculations on a simple $H_2O\cdots H_2$ model, with dihydrogen-to-oxygen distances similar to those in H_2/FER, showed that dispersion interaction energy is only of about 1 kJ mol^{-1}. Hence, it is likely that both factors (overestimated cation−dihydrogen interaction and neglected dispersion energy) approximately cancel out. To verify this, we have compared MP2 and PBE interaction energies for the $(SiH_3)_2O\cdots H_2(K^+)\cdots O(SiH_3)_2$ model at the $O\cdots H_2(K^+)\cdots O$ geometries taken from the H_2/FER. Interaction energies calculated for this model system at the MP2 and PBE levels of theory agree within 1 kJ/mol in all geometries investigated, which gives further indication that the internal errors in the PBE description of H_2/M^+−FER interactions approximately cancel out.

The thermal contribution to $\Delta U^0(T)$, and the pV term, were evaluated considering only six degrees of freedom. For the gas-phase H_2 molecule, expressions derived from the ideal gas model for translational and rotational degrees of freedom were used. For the adsorption complex, the thermal contribution was calculated from the vibrational partition function, using frequency values obtained at the harmonic approximation for the 1-T cluster model (Table 1). It should be noted, however, that for low-lying vibrational modes, the harmonic approximation can be highly inaccurate, and in addition, use of the 1-T cluster model neglects H_2 interactions with the zeolite channel wall. More precise calculations would require, first, a periodic model accounting for the gas−adsorbent interaction and, second, description of vibrational degrees of freedom at a level beyond the harmonic approximation. While such a description of the system is (at least in principle) possible, it is far beyond the scope of the present work. We would only point out that the harmonic approximation used in our theoretical study could account, at least in part, for the larger discrepancy between experimental and calculated $\Delta H°$ (100) values for H_2/K−FER, as compared to those for H_2/Na−FER (Table 2). Note that three vibrational modes with a frequency (obtained within the harmonic approximation) below 10 cm^{-1} were found for the H_2 molecule adsorbed on the 1-T cluster model (Table 1).

The nature of the $Na^+\cdots H_2$ interaction was discussed by Solans-Monfort et al.,[31] who used an energy decomposition scheme to show that the major contribution to the complex stabilization comes from polarization of the dihydrogen molecule. Only a very small charge transfer from H_2 to Na^+ was found, accounting for only a minor energy stabilization of about −0.4 kJ mol^{-1}. It is, therefore, reasonable to expect that the adsorption enthalpy correlates with corresponding changes in the H−H stretching frequency (υ). In fact, at the PBE/aug-cc-pVTZ level, the H_2 interaction energy values (without ZPE correction) calculated for Na^+/0-T, K^+/0-T, Na^+/1-T, and K^+/1-T cluster models are −16.5, −8.9, −6.7, and −3.2 kJ mol^{-1}, respectively (Table 3). Quoted in the same order, $\Delta\omega$(H−H) values (calculated within the harmonic approximation) resulted to be −91, −51, −45, and −21 cm^{-1}, thus showing a correlation between frequency shift and interaction energy.

Because the interaction energy calculated by using simple cluster models is underestimated compared to the results obtained with a more realistic periodic model (Table 2); also $\Delta\omega$(H−H) frequency shifts calculated with the 1-T cluster model should be underestimated compared to the experimental results. Indeed, the experimentally observed frequency shifts for H_2 adsorbed on Na−FER and K−FER (−63 and −52 cm^{-1}, respectively) are larger than those calculated at the PBE/aug-cc-pVTZ level by using the 1-T cluster model (−45 and −21 cm^{-1}, respectively, Table 1). This is another indication that small cluster models are not adequate for a correct analysis of the real system. There are two major sources of error in small cluster models: (i) charge transfer between metal cation and zeolite is not properly described, and (ii) the effect of the H_2 molecule interaction with the zeolite channel wall is neglected. Calculations based on the 1-T cluster model give adsorption enthalpy values (Table 2) that are too small when compared with those derived from either periodic DFT calculations or experimental measurements. By contrast, $\Delta H°$ values derived by simply considering the interaction of dihydrogen with a bare cation result in being (as expected) too large. The role of H_2 interactions with the zeolite channel wall becomes apparent from calculations of the energy barrier for rotation along the axis defined by the cation site and the center of the H_2 molecule.

TABLE 4: Experimental Thermodynamic Data (ΔH^0, KJ mol^{-1}; ΔS^0, J mol^{-1} K^{-1}) for H_2 Adsorption on Na^+ and K^+ Exchanged Zeolites

	Na−ZSM-5[a]	K−ZSM-5[a]	Na−FER[b]	K−FER[b]
$\Delta H°(100)$	−10.3 (±0.5)	−9.1 (±0.5)	−6.0 (±0.8)	−3.5 (±0.8)
ΔS^0	−121 (±10)	−124 (±10)	−78 (±10)	−57 (±10)

[a] Taken from ref 8. [b] Present work.

This barrier was evaluated in a simple way by just rotating the H_2 molecule itself, while keeping all other geometrical parameters fixed. Calculations with the 1-T cluster model gave only a very small barrier: 0.2 kJ mol^{-1}. By contrast, the rotational energy barrier calculated by using the periodic model for H_2 on Na^+ at I2/T2 site (H_2 approaching from the perpendicular channel side) was found to be 3.0 kJ mol^{-1}. Thus, it is clear that interaction of the adsorbed molecule with the zeolite framework cannot be neglected.

Finally, a comparison between results obtained for ZSM-5 and ferrierite is of interest. Table 4 summarizes the experimentally determined values of standard adsorption enthalpy and entropy ($\Delta H°$ and $\Delta S°$) for H_2 on both FER samples studied, along with corresponding results previously reported[8] for Na−ZSM-5 and K−ZSM-5. It is apparent that the interaction of H_2 with the zeolite adsorption sites is significantly stronger in ZSM-5 than in FER. This could possibly be due to the changes in the coordination number of extraframework cations with oxygen atoms of the zeolite framework. The alkali-metal sites in ZSM-5 were investigated systematically by using the combined quantum mechanical/interatomic potential function approach.[29] Numerous channel intersection sites having a low cation coordination number were found in ZSM-5. Because interaction of the hydrogen molecule with the zeolite is driven mainly by polarization due to the (net) electric charge on the alkali-metal cation, it seems reasonable to ascribe the larger H_2 adsorption enthalpy in ZSM-5 to the larger charge (smaller electron density) on the metal cation, resulting from a lower coordination number (as compared to FER). The changes in coordination of the alkali-metal cation in ZSM-5 and FER are particularly large for the K^+ ions. This is due to the fact that the K^+ ion fits very well into the eight-member ring of the entrance window of the perpendicular channel (I2/T2 site, see Figure 1). This is likely to be behind the larger decrease of the H_2 adsorption enthalpy on K^+ sites when going from ZSM-5 to FER.

It is also apparent that $\Delta S°$ values are correlated to the corresponding $\Delta H°$ values. The data available constitute too small a set to establish such a correlation firmly, but two observations support this idea. First, a definite correlation was established between $\Delta S°$ and $\Delta H°$ values for the case of CO adsorbed on several metal oxides and zeolites.[35,36] Second, a simple picture of the gas−solid interaction suggests that the less interacting the molecule, the freer it will be. From a more quantitative point of view, differences in $\Delta S°$ may be understood on the basis of the role of low-frequency motions. Entropy of gas-phase H_2 is the same for all four cases in Table 4, being that of the standard state (one atmosphere at 100 K). Hence, the observed differences in $\Delta S°$ should come from the contribution that vibrations of the adsorbed complex make to the entropy of the adsorbed state. By using low-lying vibrational frequencies calculated for the 1-T model within the harmonic approximation (Table 1), the standard eq 6 describing the vibrational entropy of a harmonic oscillator[30,37]

$$S_v = \sum_i \left(\frac{1}{T} \cdot \frac{N_A k \Theta_v^i}{e^{\Theta_v^i/T} - 1} - N_A k \cdot \ln(1 - e^{-\Theta_v^i/T}) \right) \quad (6)$$

yields 41 and 83 J mol^{-1} K^{-1} for Na−FER and K−FER, respectively. The calculated difference in $\Delta S°$ show the correct trend, and regarding H_2/Na−FER and H_2/K−FER, this difference is about twice as large as that found experimentally (Table 4). This is a reasonable agreement, considering the crudeness of the approach. Note also that, for H_2/Na−ZSM-5 and H_2/K−ZSM-5, $\Delta S°$ takes approximately the same value within experimental error in both cases. However, it is still significantly larger than that for H_2/Na−FER and H_2/K−FER, which is consistent with the larger $\Delta H°$ values for the H_2/ZSM-5 systems (Table 4).

5. Conclusions

The main conclusions of this work can be summarized as follows.

(i) By means of variable temperature IR spectroscopy, the standard adsorption enthalpy ($\Delta H°$) of molecular hydrogen on the zeolites Na−FER and K−FER was experimentally found to amount to −6.0 (± 0.8) and −3.5 (± 0.8) kJ mol^{-1}, respectively. These $\Delta H°$ values were found to agree (within ±1 kJ mol^{-1}) with those calculated by means of density functional theory (DFT) and a periodic model of the zeolite. Such an unusual (quantitative) agreement might be, however, partially fortuitous, reflecting internal cancellation of errors in the theoretical calculations (neglect of dispersion interactions and overestimation of other terms).

(ii) The adsorption enthalpy of dihydrogen on both Na−FER and K−FER is significantly smaller than corresponding values previously reported for the H_2/Na−ZSM-5 and H_2/K−ZSM-5 systems. This fact is likely due to a smaller cation coordination number (of the extraframework cation with framework oxygen atoms) in ZSM-5, as compared to FER. A larger coordination number of the alkali-metal cations in FER would result in a smaller (net) electric charge at the hydrogen adsorption site and, hence, in a smaller gas−solid interaction energy.

(iii) Calculations showed that $H_2 \cdots M^+$−FER physisorption complexes (M = Na, K) have a T-shape structure, which is also the case for the gas-phase H_2M^+ complex. Two types of alkali-metal sites were identified in FER: channel intersection sites and channel wall sites. Two hydrogen molecules can be adsorbed on the channel intersection site (one from the side of the main channel and the other one from the perpendicular channel) with nearly the same interaction strength. By contrast, only one H_2 molecule can be adsorbed on the channel wall site.

(iv) Neither the bare alkali-metal cation nor the cluster model $Al(OH)_4^-M^+$ (M = Na, K) were found to be adequate for (approximate) calculations on the interaction energy between H_2 and the (cationic) zeolite adsorbing centers. Calculations on the bare metal cation give too high an interaction energy, while the cluster model yields too-small values. It was also found that the strength of interaction of the dihydrogen molecule with the zeolite adsorbing sites depends primarily on the (net) electric charge on the metal cation. However, the adsorption complex is further stabilized by interaction of the H_2 molecule with the zeolite framework.

Acknowledgment. Work in Prague was supported by grants of ME CR no. LC512 and project Z4 055 905. The Spanish MCyT is gratefully acknowledged for supporting work done at the UIB (project nos. MAT2002-03603 and MAT2005-05350).

References and Notes

(1) Strub, A. A.; Imarisio, G. *Hydrogen as an Energy Vector*; D. Reidel: Dordrecht, The Netherlands, 1980.

(2) Weitkamp, J.; Fritz, M.; Ernst, S. *Int. J. Hydrogen Energy* **1995**, *20*, 967.

(3) van den Berg, A. W. C.; Bromley, S. T.; Jansen, J. C. *Microporous Mesoporous Mater.* **2005**, *78*, 63.

(4) Arean, C. O.; Manoilova, O. V.; Palomino, G. T.; Delgado, M. R.; Tsyganenko, A. A.; Bonelli, B.; Garrone, E. *Phys. Chem. Chem. Phys.* **2002**, *4*, 5713.

(5) Garrone, E.; Arean, C. O. *Chem. Soc. Rev.* **2005**, *34*, 846.

(6) Garrone, E.; Delgado, M. R.; Bonelli, B.; Arean, C. O. *Phys. Chem. Chem. Phys* **2005**, *7*, 3519.

(7) Arean, C. O.; Manoilova, O. V.; Bonelli, B.; Delgado, M. R.; Palomino, G. T.; Garrone, E. *Chem. Phys. Lett.* **2003**, *370*, 631.

(8) Arean, C. O.; Delgado, M. R.; Palomino, G. T.; Rubio, M. T.; Tsyganenko, N. M.; Tsyganenko, A. A.; Garrone, E. *Microporous Mesoporous Mater.* **2005**, *80*, 247.

(9) Turnes Palomino, G.; Rodriguez Delgado, M.; Tsyganenko, N. M.; Tsyganenko, A. A.; Garrone, E.; Bonelli, B.; Manoilova, O. V.; Otero Arean, C. *Stud. Surf. Sci. Catal.* **2005**, *158*, 853.

(10) Vitillo, J. G.; Damin, A.; Zecchina, A.; Ricchiardi, G. *J. Chem. Phys.* **2005**, *122*.

(11) Arean, C. O.; Manoilova, O. V.; Tsyganenko, A. A.; Palomino, G. T.; Mentruit, M. P.; Geobaldo, F.; Garrone, E. *Eur. J. Inorg. Chem.* **2001**, 1739.

(12) Perdew, J. P.; Burke, K.; Ernzerhof, M. *Phys. Rev. Lett.* **1996**, *77*, 3865.

(13) Perdew, J. P.; Burke, K.; Ernzerhof, M. *Phys. Rev. Lett.* **1997**, *78*, 1396.

(14) Blochl, P. E. *Phys. Rev. B* **1994**, *50*, 17953.

(15) Kresse, G.; Joubert, D. *Phys. Rev. B* **1999**, *59*, 1758.

(16) Kresse, G.; Hafner, J. *Phys. Rev. B* **1993**, *48*, 13115.

(17) Kresse, G.; Hafner, J. *Phys. Rev. B* **1994**, *49*, 14251.

(18) Kresse, G.; Furthmuller, J. *Phys. Rev. B* **1996**, *54*, 11169.

(19) Kresse, G.; Furthmuller, J. *Comp. Mater. Sci.* **1996**, *6*, 15.

(20) Bludsky, O.; Silhan, M.; Nachtigall, P.; Bucko, T.; Benco, L.; Hafner, J. *J. Phys. Chem. B* **2005**, *109*, 9631.

(21) Vaughan, P. A. *Acta Crystallogr.* **1966**, *21*, 983.

(22) It should be pointed out that this numbering scheme differs from that used in Database of Zeolite Structures: http://www.iza-structure.org/databases/, where T1 and T4 positions are switched.

(23) Dunning, T. H. *J. Chem. Phys.* **1989**, *90*, 1007.

(24) Woon, D. E.; Dunning, T. H. *J. Chem. Phys.* **1993**, *98*, 1358.

(25) Frisch, M. J.; Trucks, G. W.; Schlegel, H. B.; Scuseria, G. E.; Robb, M. A.; Cheeseman, J. R.; Montgomery, J. A., Jr.; Vreven, T.; Kudin, K. N.; Burant, J. C.; Millam, J. M.; Iyengar, S. S.; Tomasi, J.; Barone, V.; Mennucci, B.; Cossi, M.; Scalmani, G.; Rega, N.; Petersson, G. A.; Nakatsuji, H.; Hada, M.; Ehara, M.; Toyota, K.; Fukuda, R.; Hasegawa, J.; Ishida, M.; Nakajima, T.; Honda, Y.; Kitao, O.; Nakai, H.; Klene, M.; Li, X.; Knox, J. E.; Hratchian, H. P.; Cross, J. B.; Bakken, V.; Adamo, C.; Jaramillo, J.; Gomperts, R.; Stratmann, R. E.; Yazyev, O.; Austin, A. J.; Cammi, R.; Pomelli, C.; Ochterski, J. W.; Ayala, P. Y.; Morokuma, K.; Voth, G. A.; Salvador, P.; Dannenberg, J. J.; Zakrzewski, V. G.; Dapprich, S.; Daniels, A. D.; Strain, M. C.; Farkas, O.; Malick, D. K.; Rabuck, A. D.; Raghavachari, K.; Foresman, J. B.; Ortiz, J. V.; Cui, Q.; Baboul, A. G.; Clifford, S.; Cioslowski, J.; Stefanov, B. B.; Liu, G.; Liashenko, A.; Piskorz, P.; Komaromi, I.; Martin, R. L.; Fox, D. J.; Keith, T.; Al-Laham, M. A.; Peng, C. Y.; Nanayakkara, A.; Challacombe, M.; Gill, P. M. W.; Johnson, B.; Chen, W.; Wong, M. W.; Gonzalez, C.; Pople, J. A. *Gaussian 03*; Gaussian, Inc.: Wallingford, CT, 2004.

(26) Boys, S. F.; Bernardi, F. *Mol. Phys.* **1970**, *19*, 553.

(27) Nachtigallova, D.; Nachtigall, P.; Sierka, M.; Sauer, J. *Phys. Chem. Chem. Phys.* **1999**, *1*, 2019.

(28) Nachtigall, P.; Davidova, M.; Nachtigallova, D. *J. Phys. Chem. B* **2001**, *105*, 3510.

(29) Kucera, J.; Nachtigall, P. *Phys. Chem. Chem. Phys.* **2003**, *5*, 3311.

(30) McQuarrie, D. A. *Statistical Mechanics*; Harper Collins: New York, 1976.

(31) Solans-Monfort, X.; Branchadell, V.; Sodupe, M.; Zicovich-Wilson, C. M.; Gribov, E.; Spoto, G.; Busco, C.; Ugliengo, P. *J. Phys. Chem. B* **2004**, *108*, 8278.

(32) Bordiga, S.; Palomino, G. T.; Paze, C.; Zecchina, A. *Microporous Mesoporous Mater.* **2000**, *34*, 67.

(33) Bludsky, O.; Nachtigallova, D.; Bulanek, R.; Nachtigall, P. *Stud. Surf. Sci. Catal.* **2005**, *158*, 625.

(34) Bukowski, R.; Jankowski, P.; Jeziorski, B.; Jeziorski, M.; Kucharski, S. A.; Moszynski, R.; Rybak, S.; Szalewicz, K.; Williams, H. L.; Wormer, P. E. S. *An Ab Initio Program for Many-Body Symmetry-Adapted Perturbation Theory Calculations on Intermolecular Interaction Energies*; University of Delaware and University of Warsaw, 1996.

(35) Garrone, E.; Fubini, B.; Bonelli, B.; Onida, B.; Arean, C. O. *Phys. Chem. Chem. Phys.* **1999**, *1*, 513.

(36) Garrone, E.; Bonelli, B.; Tsyganenko, A. A.; Delgado, M. R.; Palomino, G. T.; Manoilova, O. V.; Arean, C. O. *J. Phys. Chem. B* **2003**, *107*, 2537.

(37) Symbols used in eq 6 are the same as those used in eq 1.